Biochemical and Biophysical Research Communications 437 (2013) 217–224

Contents lists available at SciVerse ScienceDirect

Biochemical and Biophysical Research Communications

journal homepage: www.elsevier.com/locate/ybbrc

MicroRNA-124 targets CCNA2 and regulates cell cycle in STHdh^{Q111}/Hdh^{Q111} cells

Eashita Das [a], Nihar Ranjan Jana [b], Nitai Pada Bhattacharyya [a,*]

[a] Crystallography and Molecular Biology Division, Saha Institute of Nuclear Physics (SINP), 1/AF Bidhan Nagar, Kolkata 700 064, India
[b] National Brain Research Centre, Manesar, Haryana 122 050, India

ARTICLE INFO

Article history:
Received 8 June 2013
Available online 21 June 2013

Keywords:
Huntington's disease
MicroRNA-124
Cyclin A2
Cell cycle
STHdh^{Q7}/Hdh^{Q7} cells
STHdh^{Q111}/Hdh^{Q111} cells

ABSTRACT

Mutation in *huntingtin* (*HTT*) gene causes Huntington's disease (HD). Expression of many micro RNAs is known to alter in cell, animal models and brains of HD patients, but their cellular effects are not known. Here, we show that expression of microRNA-124 (miR-124) is down regulated in HD striatal mutant STHdh^{Q111}/Hdh^{Q111} cells, a cell model of HD compared to STHdh^{Q7}/Hdh^{Q7} cells. STHdh^{Q7}/Hdh^{Q7} and STHdh^{Q111}/Hdh^{Q111} cells express endogenously full length wild type and mutant *HTT* respectively. We confirmed this result in R6/2 mouse, an animal model of HD, expressing mutant *HTT*. Gene Ontology terms related to cell cycle were enriched significantly with experimentally validated targets of miR-124. We observed that expression of Cyclin A2 (CCNA2), a putative target of miR-124 was increased in mutant STHdh^{Q111}/Hdh^{Q111} cells and brains of R6/2 mice. Fraction of cells in S phase was higher in asynchronously growing mutant STHdh^{Q111}/Hdh^{Q111} cells compared to wild type STHdh^{Q7}/Hdh^{Q7} cells and could be altered by exogenous expression or inhibition of miR-124. Exogenous expression or knock down of CCNA2, a target of miR-124, also alters proportion of cells in S phase of HD cell model. In summary, decreased miR-124 expression could increase CCNA2 in cell and animal model of HD and is involved in deregulation of cell cycle in STHdh^{Q111}/Hdh^{Q111} cells.

1. Introduction

MicroRNAs (miRNAs) belong to a class of small non-coding RNA, approximately 21 nucleotides long. Mature miRNA interacts with 3′-untranslated (3′-UTR) regions of genes and down-regulates the targets either by degrading mRNA or inhibiting translation. By regulating diverse targets, miRNA participates in various biological processes including cell death and proliferation [1], differentiation [2], development [3,4] and cell cycle [5–7]. Alterations of miRNA expressions have been implicated in many diseases including neurodegenerative diseases and cancers [8]. Various miRNAs are altered in cell model [9], animal model [10] and post mortem brains of HD [11,12]. We have shown that among these miRNAs, miR-146a targets *TBP* [9], miR-125b, miR-146a, miR-150, miR-214 target *HTT* and miR-150 targets *TP53* [13,14]. Analyzing the validated targets of 54 altered miRNAs in brains of HD patients, we have shown earlier that cell cycle related Gene Ontology terms were significantly enriched with the validated targets of these miRNAs [15] indicating possible involvement of deregulated miRNAs in cell cycle.

Reactivation of cell cycle has been proposed to cause neurodegeneration in many diseases including HD. Increased phosphorylation of Rb, expression of E2F-1 and decreased expression of p27 in tissues from transgenic mice or postmortem brains of HD patients indicate possible reactivation of cell cycle in HD [16–19]. Alteration of cell cycle in cells expressing mutant *HTT* has not yet been shown. It is difficult to show alteration of cell cycle directly in brain tissue. So, in the present manuscript, we utilized conditionally immortalized striatal mouse STHdh^{Q111}/Hdh^{Q111} cells that express full-length mutant *HTT* from chromosomal region at physiological level [20] to show deregulation of cell cycle and also decreased mir-124 expression might involve in such deregulation by targeting CCNA2.

2. Materials and methods

2.1. R6/2 mice, STHdh^{Q7}/Hdh^{Q7} and STHdh^{Q111}/Hdh^{Q111} cells

We obtained paraffin embedded cryosection with 20 μm thickness from R6/2 and control mice as described earlier. R6/2 mice, expressing HD exon 1 gene with ~150 CAG repeats in the pathological range, considered to be an animal model of HD [14].

Abbreviations: 3′-UTR, 3′-untranslated region; CCNA2, Cyclin A2; HD, Huntington's disease; miRNA, micro RNA.

* Corresponding author. Fax: +91 033 23374637.
E-mail addresses: nitaipada.bhattacharya@saha.ac.in, nitai.bhattacharyya@gmail.com (N.P. Bhattacharyya).

0006-291X/$ - see front matter © 2013 Elsevier Inc. All rights reserved.
http://dx.doi.org/10.1016/j.bbrc.2013.06.041

Conditionally immortalized striatal neuronal progenitor STHdh^{Q7}/Hdh^{Q7} and STHdh^{Q111}/Hdh^{Q111} cells express full-length wild type *HTT* with 7Q (homozygous) and full length mutated *HTT* with 111Q (homozygous) from chromosomal region respectively and is considered as a model for HD. These cell lines were established from wild type and homozygous mutant Hdh knock in mice respectively [20]. This cell model has been widely used for identification of gene expression abnormalities and other molecular defects in HD.

2.2. Cell culture

STHdh^{Q7}/Hdh^{Q7} and STHdh^{Q111}/Hdh^{Q111} cells were cultured as described previously [14].

2.3. Expression plasmids

Precursor miRNA sequences (chr8: 9760898–9760982,-strand) of mature miR-124 was amplified by PCR from human genomic DNA and cloned into vector pRNA-U61.Hygro (Genscript, USA) using restriction enzymes *BamHI* and *HindIII* (NEB, USA) sites. Precursor miRNA is denoted by pre-mir-124 while mature miRNA is represented by miR-124. Primers used to amplify pre-mir-124 were: Forward Primer: 5′-*CGCGGATC*CATCAAGATTAGAGGCTCTGC-3′ and Reverse Primer: 5′-*CCCAAGCTT*AAAAAATTCAAGTGCAGCCG-TAGGCT-3′. Italics sequences were adaptors for cloning. Mature miR-124 sequence is conserved in human and mouse, Predicted recognition site of miR-124 at 3′-UTR of mouse CCNA2 gene (position 765–784) was amplified using forward primer 5′-*CGACGCGT*-CAC ACACACAGAGATCC ACCA-3′ and reverse primer 5′-*CCCAAGCTT*CAGACCAGTGCAAACCAGAA-3′ using genomic DNA form STHdh^{Q111}/Hdh^{Q111} cells as template. PCR product was cloned into pMIR-REPORT Luciferase vector (Ambion, USA) using *MluI* and *HindIII*. Full-length mouse CCNA2 was cloned into pEGFPC2 (BD Biosciences) vector from RNA isolated using Neuro2A cells following methods described earlier [21]. Mouse CCNA2 gene specific primers used to clone were Forward primer: 5′-*ACGCGTC-GACG*CCTGCTCTCGCTGCATCA-3′ and reverse primer 5′-*CGGG-ATCC*CACTTAGTGTCTCTGGGTTG-3′.

2.4. Knock-down of mouse CCNA2 by siRNA

Knock down of CCNA2 in mouse cells by sequence specific siRNA was carried out following methods described earlier [22]. Briefly, DNA sequence 391-CCACTGACACCTCTTGACT-410 of mouse CCNA2 (gi|161353443|ref|NM_009828) was used for designing siRNA using the online software from GenScript (https://www.genscript.com/ssl-bin/app/rnai website). The complete sequence inserted into the expression vector pRNA-Hygro/U6.1was 5′-GCCACTGACACCTCTTGACT*TTCAAGAGA*AGTCAAGAGGTGTCAGTGG-TTT TTTCCAA-3′ (designated as 'siCCNA2') with termination signal and appropriate restriction site linkers (*BanHI* and *HindIII*, not shown) and an insert for loop sequence (italics). Non-silencing control (scramble siCCNA2 sequence) with random nucleotides 5′-AGCACTTATACCTCGCCTC-3′ was designed using Genscript sequence scrambler tool. Complete sequence of scramble siCCNA2 was 5′-CGGGATCCCAGCACTTATACCTCGCCTCTTGATATCCG GAG-GCGAGGTATAA GTGCTTTTTTTCCAAAAGCTTGGG-3′ was cloned in the same vector as described above. Scrambled siCCNA2 and siCCNA2 clones were transfected in STHdh^{Q7}/Hdh^{Q7} and STHdh^{Q111}/Hdh^{Q111} cells separately using Lipofectamine 2000 (Invitrogen, USA) following manufacturer's protocol. Knock down of CCNA2 in these cells was confirmed by western blot analysis using anti CCNA2 antibody.

2.5. Transfection

Transient transfcetion of cloned pre-miRNA, luciferase reporter vectors with 3′-UTR for recognition site of miR-124 [14,15] and GFP tagged CCNA2 was carried out using Lipofectamine 2000 (Invitrogen, USA) as described earlier. Transfection efficiency for GFP-CCNA2 was monitored by counting GFP+ cells under fluorescence microscope [22] and by FACS. Transfection efficiency ranged from 70% to 80%.

2.6. Flow cytometry

STHdh^{Q7}/Hdh^{Q7} and STHdh^{Q111}/Hdh^{Q111} cells were prepared for flow cytometry according to the protocol as described earlier [23]. DNA was stained using 50 μg/ml propidium iodide (PI) for 15 min. PI fluroscence was monitored with FACS calibur flow cytometry (Becton Dickinsion) fitted with 488 nm laser. To minimize the spectral overlap of CCNA2-GFP clone, 7-Aminoactinomycin D (7-AAD) was used for DNA staining. At least 25,000 cells were collected and analyzed with CellQuest software. Cell cycle distributions were calculated with Modfit LT software.

2.7. RNA preparation

Total RNA was extracted from cultured cells using Trizol Reagent (Invitrogen, USA) according to manufacturer's protocol [9]. We prepared RNA from these paraffinized tissue using the protocol as described earlier [14].

2.8. Quantitative real-time reverse transcription PCR (qRT-PCR) for gene and miR-124

Total cellular RNA (1 μg) was reverse transcribed according to the procedure as described earlier [9,13]. The Ensemble ID of mouse CCNA2 is ENSMUST00000029270.

Primer sequence used to detect mouse CCNA2 mRNA expression:

Forward primer: 5′TGCAGCCTGCAAACTGTAAGG3′.
Reverse primer: 5′GCAGCTCCAGCAATGAGTGAA3′.

Primer sequence used to detect mouse CHK1 mRNA expression:

Forward primer: 5′ATTCTGCTCCTCTGGCTTTGC3′.
Reverse primer: 5′TGGCCTCTTTGCTCCTCTGTT3′.

Primer sequence used to detect β-Actin expression:

Forward primer: 5′ TCCTGTGGCATCCACGAAACT3′.
Reverse primer: 5′ GAAGCATTTGCGGTGGAC3′.

In the present work, we used β-Actin for the normalization of mRNA expression.

Methods for detection of miR-124 was similar to method described earlier [9,13] using commercially available miR-124 specific Taqman primers and PCR master mix (AB, USA). Mir-17-5p and beta-actin was used as endogenous control. The fold changes were calculated as per SDS software V 2.0.

2.9. Western blot analysis

Methods for protein isolation from cultured cells or paraffin embedded tissues were similar to method published elsewhere [9,13,24]. Membranes were incubated with anti-CCNA2 antibody (Cell Signaling Technologies) at 1:1000 dilutions and CHK1 antibody (Santa Cruz Biotechnology) at 1:500 dilutions for overnight

at 4 °C. CCNA2 and CHK1 protein level was detected by horseradish peroxidase (HRP) conjugated mouse and rabbit secondary antibody respectively (Genei, Bangalore).

2.10. Luciferase assays

Reporter luciferase activities were determined following the methods described earlier [9,14]. STHdh^{Q111}/Hdh^{Q111} cells were plated the day before transfection at 5×10^4 cells per well in 24-well plates (Nunc, USA). The 3′-UTR sequence of mouse CCNA2 containing miR-124 binding site was transfected in STHdh^{Q111}/Hdh^{Q111} cells together with 300 ng of cloned pre-mir-124 using Lipofectamine 2000 (Invitrogen, USA). Forty-eight hours after transfection, cells were harvested and luciferase assays were performed.

2.11. Enrichment analysis for Gene Ontology

We have used GeneCodis3 [25] as described earlier [23] for enrichment analysis of Gene Ontology for biological processes and Kyoto Encyclopedia of Genes and Genomes (KEGG) pathway. Level of significance was provided by the software after correction for multiple testing.

2.12. Image processing

Images of histograms, western blots and cell cycle distributions were prepared with the help of Adobe photoshop CS2 software.

2.13. Statistical analysis

Data are presented as mean ± standard deviation. Statistical significance was determined by student's unpaired *t*-test using Graph Pad Software, QuickCalcs, (http://www.graphpad.com/quickcalcs/index.cfm).

3. Results

3.1. Decreased expression of miR-124 in STHdh^{Q111}/Hdh^{Q111} cells and in striatum of R6/2 mice

We observed that expression of miR-124 was decreased significantly in STHdh^{Q111}/Hdh^{Q111}cells (Fig. 1A). Expression of miR-124 was also decreased in cortex and striatum of 8 weeks old R6/2 mice compared to mice of same strain and age but this decrease was not statistically significant. However, in 16 weeks old R6/2 mice, expression of miR-124 decreased significantly (Fig. 1B). Taken together, we showed here that expression of miR-124 was decreased in STHdh^{Q111}/Hdh^{Q111} cells, cortex and striatum regions of 16 weeks old R6/2 mice brain.

3.2. Enrichment of Gene Ontology terms with validated targets of miR-124

We collected from various resources including published data for experimentally validated targets of miR-124 (Supplementary Table S1A). We determined the enrichment of validated targets of miR-124 using freely available software GeneCodis3 [25]. It was revealed that GO terms cell cycle (GO: 0007049), cell division

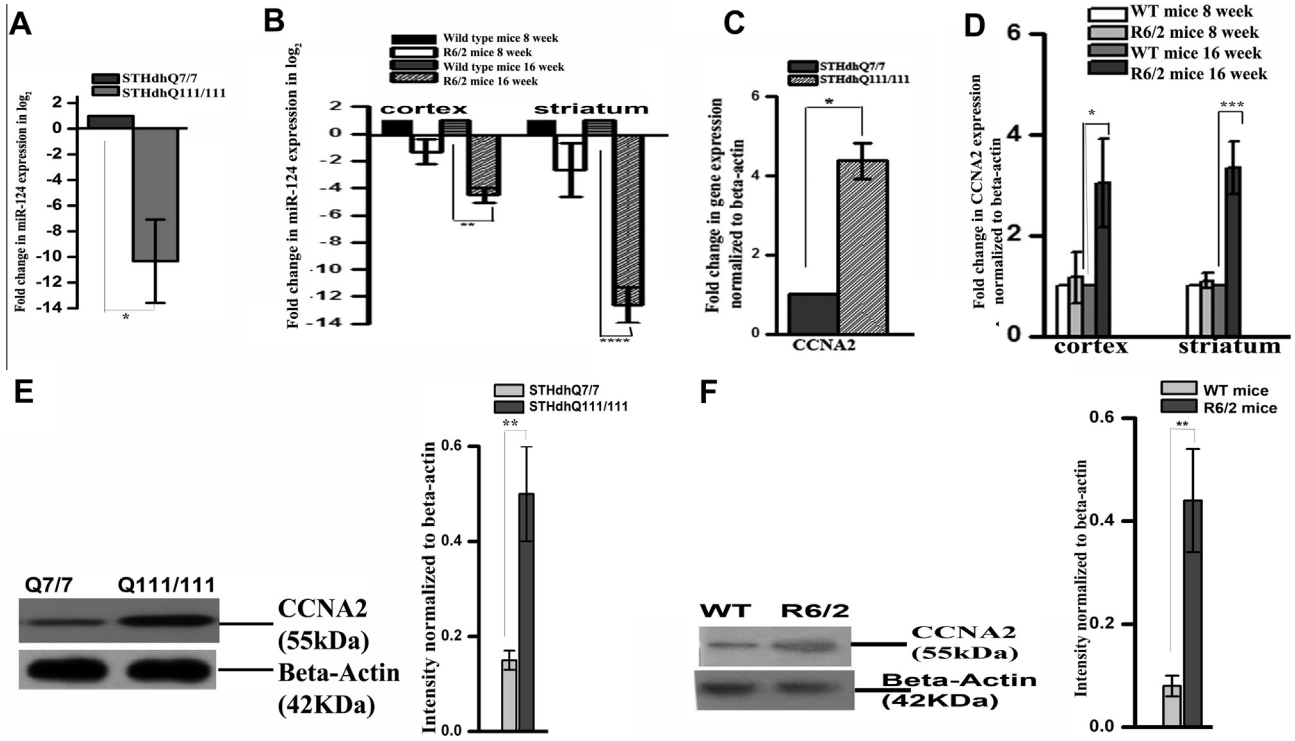

Fig. 1. Expression of miR-124 and its predicted target CCNA2 in cell and animal model of HD. (A) Expression of mature miR-124 by Q-RT PCR for mature miRNA using stem-loop specific primers available commercially. Fold changes in $\log_2$ shown with respect to STHdh^{Q7}/Hdh^{Q7}cells. (B) Expression of miR-124 in cortex and striatum of 8 weeks and 16 weeks old R6/2 mice compared to age matched control mice following the methods described in (A). (C) Expression of CCNA2 mRNA in STHdh^{Q111}/Hdh^{Q111} cells normalized with expression of β-actin and compared with expression of CCNA2 in STHdh^{Q7}/Hdh^{Q7} cells. (D) Expression CCNA2 mRNA in cortex and striatum of R6/2 mice compared to age matched control mice. (E) Expression of CCNA2 protein in STHdh^{Q111}/Hdh^{Q111} and STHdh^{Q7}/Hdh^{Q7}cells and average of densitometric values of the band intensities (right panel) normalized with the value obtained with β-actin. (F) Representative result of the Western blot and average of intensities for CCNA2 protein in striatum of 16 weeks old R6/2 mouse and age matched control mouse (right panel). Error bars represent standard deviations of the values obtained in 3 independent experiments. *, **, *** and **** represent level of significance $p \leqslant 0.05$, $p \leqslant 0.01$, $p \leqslant 0.001$ and $p \leqslant 0.0001$ respectively.

(GO: 0051301), negative regulation of cell proliferation (GO:0008285), mitosis (GO:0007067) and G2-M transition DNA damage checkpoint (GO:0031572) related to cell cycle were enriched with 25 unique proteins (ACTR8, AHR, APEX2, B4GALT1, BTG3, CAV1, CCDC99, CD164, CDC14B, CDCA7, CDK2, CDK4, CDK6, CEBPA, DHCR24, E2F6, GNAI3, ITGB1, KATNA1, MAD2L2, NEK6, NEK9, RARG, TWIST2 and UHRF1) significantly ($p \leqslant 0.0059$). KEGG pathway "cell cycle (KEGG: 04110)" was also significantly enriched ($p = 0.0045$). This result shows that miR-124 targets many proteins to regulate cell cycle (Supplementary Tables S1B and S1C).

3.3. Endogenous mRNA expression of CCNA2 in STHdh^{Q111}/Hdh^{Q111} cells and striatum of R6/2 mice

Expression of miR-124 was decreased in cell and animal model of HD and predicted to target CCNA2. It is expected that endogenous expression of CCNA2 would increase in HD models, if miR-124 actually target the gene. It was observed that expression of CCNA2 mRNA was indeed increased in STHdh^{Q111}/Hdh^{Q111} cells compared to STHdh^{Q7}/Hdh^{Q7} cells (Fig. 1C) and in cortex and striatum of 16 weeks old R6/2 mice (Fig. 1D) compared to cortex and striatum of age matched control mice respectively. Similar increase in expression of CCNA2 protein was also observed in STHdh^{Q111}/Hdh^{Q111} cells (Fig. 1E) and striatum of 16 weeks old R6/2 mice brain (Fig. 1F). Inverse correlation of expression of miR-124 and its predicted target gene in cell and animal model of HD indicates that CCNA2 could be a real target of miR-124.

3.4. CCNA2 is a target of miR-124

Expression of endogenous CCNA2 mRNA (Fig. 2A) and protein (Fig. 2B) was decreased in STHdh^{Q111}/Hdh^{Q111}cells expressing pre-mir-124 exogenously. Expression of pre-mir-124 increased expression of mature miR-124 (data not shown). This result shows that miR-124 may target CCNA2. We also observed that endogenous expression of CCNA2 mRNA (Fig. 2C) and protein (Fig. 2D) was increased in presence of miR-124 inhibitor (Ambion, USA) in STHdh^{Q7}/Hdh^{Q7} cells. Recognition site of miR-124 at 3′-UTR of mouse CCNA2 is shown in Fig. 2E. We constructed the 3′-UTR of mouse CCNA2 with recognition site for miR-124 in lusiferase pmir-Reporter vector (Ambion, USA). Transfection of this reporter vector in STHdh^{Q7}/Hdh^{Q7} and STHdh^{Q111}/Hdh^{Q111} cells resulted in significantly increased luciferase activities in STHdh^{Q111}/Hdh^{Q111}

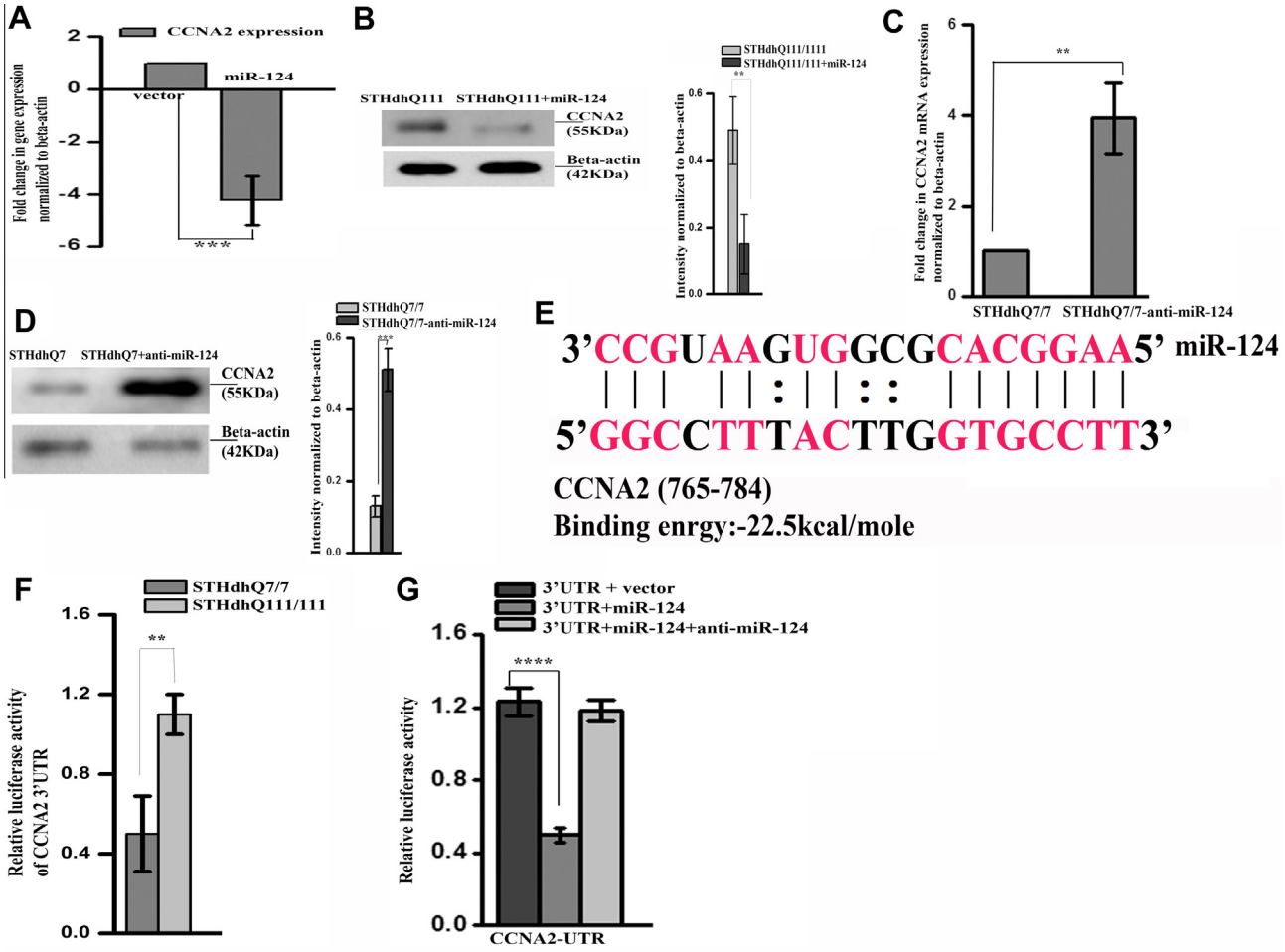

Fig. 2. Effects of exogenous expression of pre-mir-124 on CCNA2 expression and reporter luciferase activities. (A) Decreased expression of CCNA2 mRNA detected by RT-PCR and (B) Expression of CCNA2 protein by western blot in STHdh^{Q111}/Hdh^{Q111} cells expressing pre-mir-124 exogenously. Expression of CCNA2 in same cell expressing the empty U61 vector was used as control. Intensity compared to β-actin was shown in right panel of representative immunoblot. (C) Effect of inhibition of miR-124 by anti-miR-124 in STHdh^{Q7}/Hdh^{Q7} cells on CCNA2 mRNA and (D) protein expression. Average of intensities of the bands for CCNA2 is also shown in the right panel (D). (E) Microcosm predicted pairing of miR-124 to the 3′UTR of the mouse CCNA2gene. (F) Activities of luciferase reporter containing the 3′UTR sequence of CCNA2 having the predicted recognition site of miR-124 in STHdh^{Q111}/Hdh^{Q111} and STHdh^{Q7}/Hdh^{Q7} cells. Normalization of protein level was performed by taking ratio of Relative Luciferase Units (RLU) of cloned constructs and empty vector. (G) Reporter luciferase activities in STHdh^{Q111}/Hdh^{Q111} cells expressing pre-mir-124 and anti-miR-124 together. Error bars represent standard deviations of the values obtained in three independent experiments. **, *** and **** represent level of significance $p \leqslant 0.01$, $p \leqslant 0.001$ and $p \leqslant 0.0001$ respectively.

cells compared to STHdh^{Q7}/Hdh^{Q7} cells (Fig. 2F). Co-transfection of 3′-UTR of CCNA2 cloned in luciferase vector and pre-mir-124 in STHdh^{Q111}/Hdh^{Q111} cells, decreased the reporter luciferase activity significantly. However, treatment with inhibitor of miR-124 in these cells inhibited such reduction in reporter luciferase activity (Fig. 2G). Taking together, we showed that CCNA2 is a target of miR-124.

3.5. Effects of cell cycle distributions by exogenous expression and inhibition of miR-124

Comparison of distributions of asynchronously growing STHdh^{Q111}/Hdh^{Q111} and STHdh^{Q7}/Hdh^{Q7} cells in different phases of cell cycle revealed that significantly increased proportions of cells in S phase ($p = 0.008$, $n = 4$) and G2-M phase ($p = 0.0005$, $n = 4$) in STHdh^{Q111}/Hdh^{Q111} cells (Fig. 3A). Exogenous expression of pre-mir-124 in STHdh^{Q111}/Hdh^{Q111} cells significantly increased ($p \leqslant 0.001$, $n = 4$) proportion of cells in G0–G1 phase (56.0 ± 0.6)% compared to empty vector U61 transfected STHdh^{Q111}/Hdh^{Q111} cells (39.9 ± 0.3)% (Fig. 3B). Significant decrease in proportion of cells in S phase from (44.9 ± 0.2)% to (35.2 ± 0.8)%, ($p < 0.05$ and $n = 4$) was also evident in such condition. Inhibition of miR-124 expression in STHdh^{Q7}/Hdh^{Q7} cells increased significantly ($p \leqslant 0.001$, $n = 4$) the proportion of cells in S phase from (43.8 ± 0.4)% to (53.5 ± 1.1)% (Fig. 3C). This result shows that miR-124 altered the proportion of cells in the G1 and S phase.

3.6. Effects of CCNA2 on cell cycle distribution in STHdh^{Q7}/Hdh^{Q7} and STHdh^{Q111}/Hdh^{Q111} cells

We have knocked down CCNA2 in STHdh^{Q111}/Hdh^{Q111} cells to identify role of CCNA2 in cell cycle deregulation. Expression of 'SiC-CNA2' in STHdh^{Q111}/Hdh^{Q111} cells resulted in significant ($p < 0.05$, $n = 3$) decreased expression of CCNA2 mRNA and CCNA2 protein, whereas expression of scrambled siRNA 'scrCCNA2' did not alter expression of CCNA2 mRNA (Fig. 4A) and protein (Fig. 4B). When CCNA2 was knocked down in STHdh^{Q111}/Hdh^{Q111} cells, proportion of cells in S phase decreased ($p = 0.006$, $n = 3$) and concomitantly

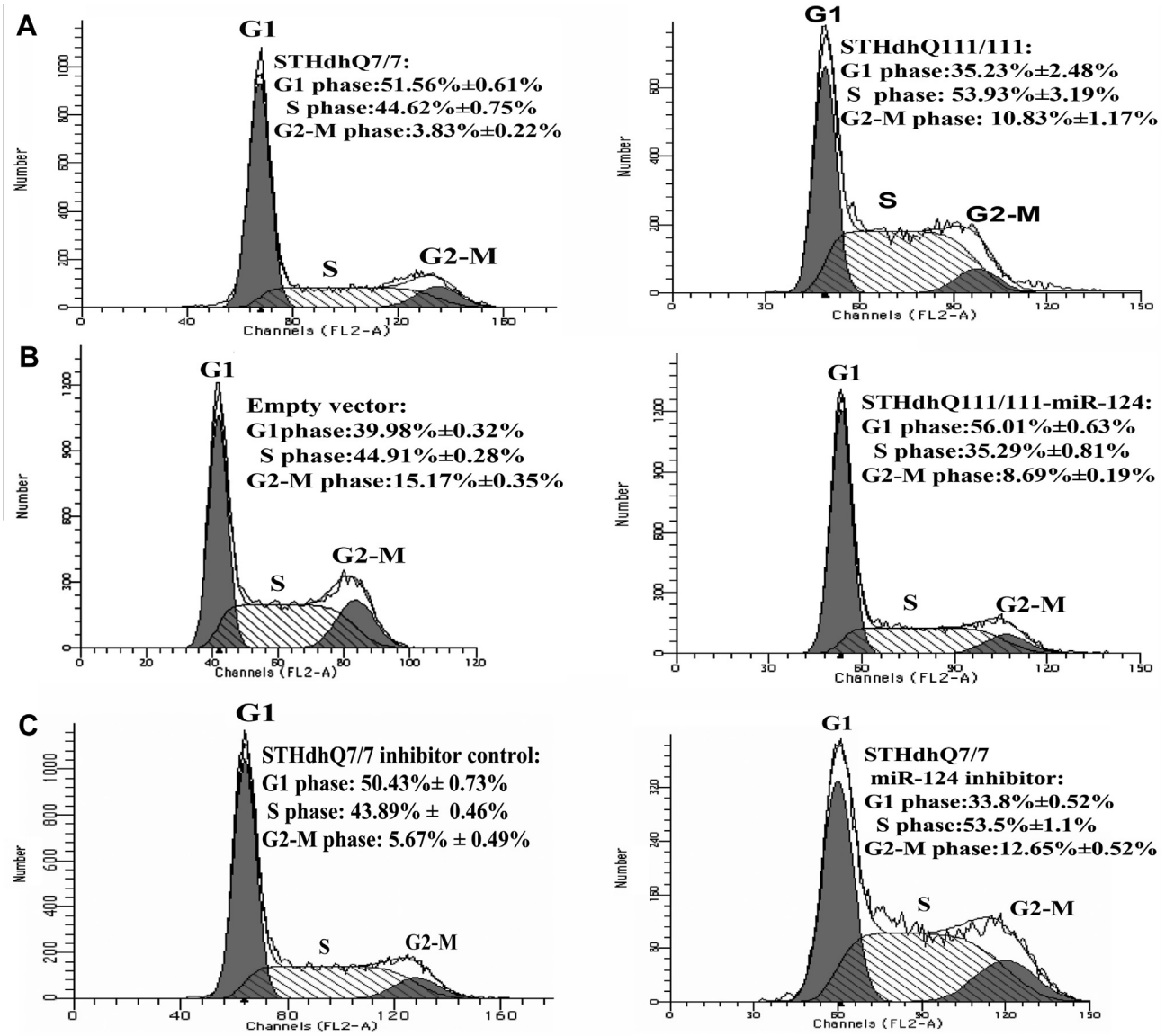

Fig. 3. Effects of miR-124 and its inhibitors on cell cycle distribution of asynchronously growing HD cell model. (A) Cell cycle distribution in STHdh^{Q7}/Hdh^{Q7} and STHdh^{Q111}/Hdh^{Q111}. (B) Cell cycle distribution of STHdh^{Q111}/Hdh^{Q111} cells expressing pre-mir-124. (C) Cell cycle distribution in STHdh^{Q7}/Hdh^{Q7} cells treated with anti-miR-124. Inset numbers indicate different phases of cell cycle distribution from four independent experiments. *P* value and level of significance is mentioned in main text.

G0–G1 phase cells increased significantly ($p = 0.001$, $n = 3$) (Fig. 4C). We have transiently expressed CCNA2 in STHdh^{Q7}/Hdh^{Q7} cells, as the expression of CCNA2 was lower compared to STHdh^{Q111}/Hdh^{Q111} cells that increased CCNA2 mRNA and protein (data not shown). Exogenous expression of CCNA2 in STHdh^{Q7}/Hdh^{Q7} cells, significantly increased ($p = 0.001$, $n = 3$) proportion of cells in S phase (Fig. 4D) as well as check point protein CHK1 mRNA and protein expression (Fig. 4E).

To exclude cell type specificity of modulation of cell cycle by CCNA2, we have transiently expressed CCNA2 in Hela cells and concomitant increase of CCNA2 mRNA and protein expression was observed. Ectopic overexpression of CCNA2 causes similar increase in S phase cell population in HeLa cells (Supplementary Figure S1). These results confirmed our hypothesis that CCNA2, a target of miR-124, may play a pivotal role in cell cycle regulation of STHdh^{Q111}/Hdh^{Q111} cells.

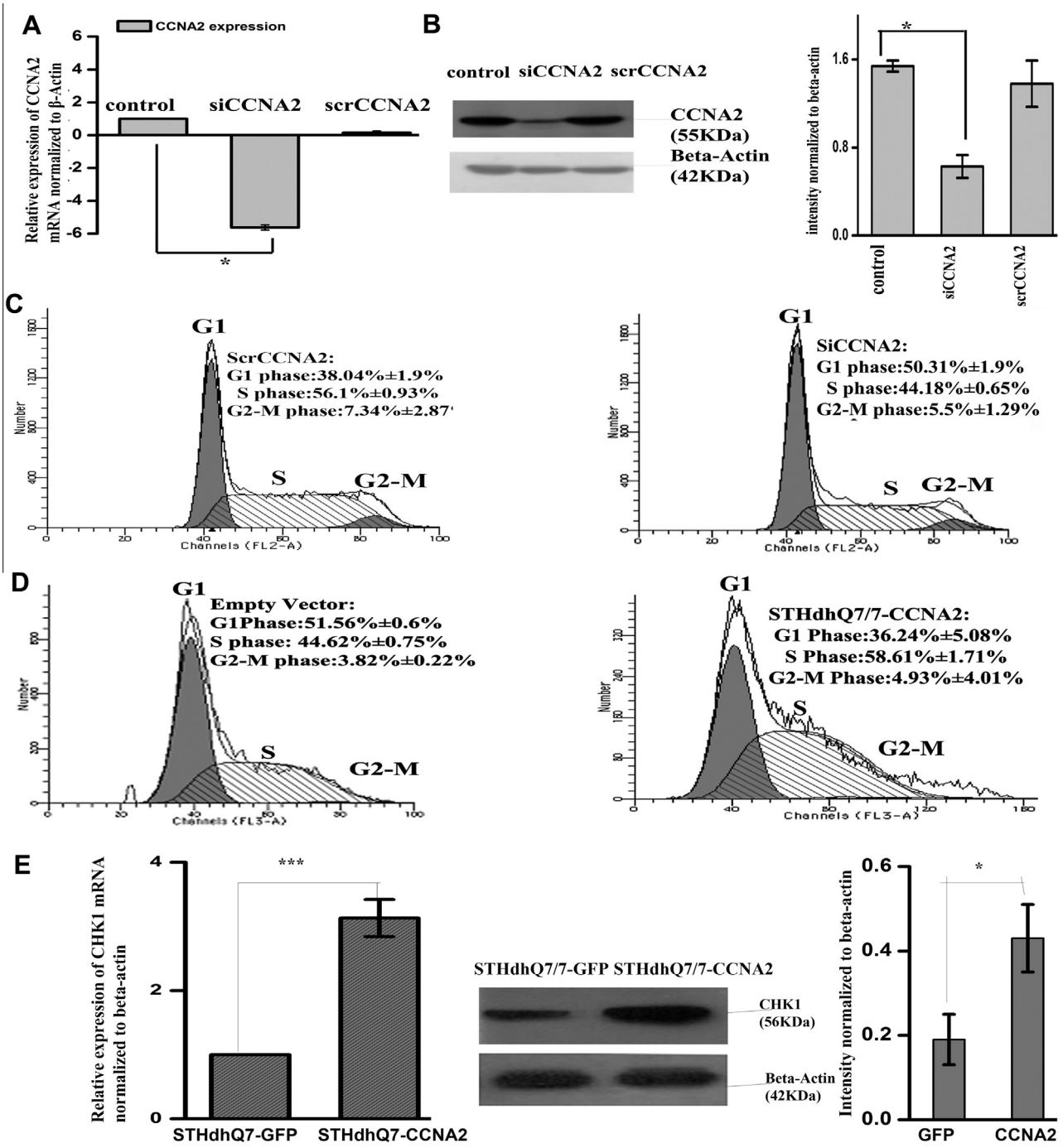

Fig. 4. Effects of cell cycle distribution by altering the expression of CCNA2. (A) Expression of CCNA2 mRNA normalized with expression of β-actin and (B) Representative immunoblots and the intensities of bands corresponding to CCNA2 protein and β-actin in STHdh^{Q111}/Hdh^{Q111} cells expressing the siCCNA2 and control scrambled siRNA (scrCCNA2). (C) Effects of knocking down CCNA2 in STHdh^{Q111}/Hdh^{Q111} cells on the cell cycle distribution. (D) Cell cycle distribution in STHdh^{Q7}/Hdh^{Q7} cells over expressing GFP-CCNA2 and the empty vector GFP separately. (E) Overexpression of GFP-CCNA2 into STHdh^{Q7}/Hdh^{Q7} cells increased CHK1 mRNA and protein compared to GFP transfected STHdh^{Q7}/Hdh^{Q7} cells and relative band intensities were determined by densitometry. Significance level is shown in results section.

4. Discussion

We demonstrated that expression of miR-124 that targets CCNA2 is decreased in a cell model and an animal model of HD and alters distributions of cells in different phases of cell cycle in asynchronously growing STHdh^{Q111}/Hdh^{Q111} cells compared to STHdh^{Q7}/Hdh^{Q7} cells. These cell lines were derived from embryonic striatal primordia of Hdh^{Q111} homozygous CAG 111 knock-in and wild type littermate respectively. In these cell lines, *HTT* is expressed by endogenous promoter at physiological level. STHdh^{Q111}/Hdh^{Q111} cells represent HD and show many features of the disease [20]. This cell model has been widely used to identify altered gene expression [26–28]. Significant down regulation of miR-124 and subsequent up regulation of CCNA2 were observed in cortex as well as striatum of 16 weeks old R6/2 mice compared to 8 weeks old R6/2 mice as well as age matched wild type counterparts, indicating such decrease was associated with gradual progression of the disease, consistent with earlier report [29].

Expression of miR-124, regulated by NRSF/REST [12], has been shown to decrease in brains of HD patients [10]. Decreased expression of miR-124 in STHdh^{Q111}/Hdh^{Q111} could be explained by increased expression of NRSF/REST in same cells, we reported earlier [30]. We observed that alterations of miR-124 expression changed the proportion of cells in different phases of cell cycle by targeting CCNA2. It has been proposed that a miRNA may exert its effect by targeting many genes of a common pathway [31]. Our bioinformatics analysis revealed that miR-124 could actually target 25 proteins related to cell cycle (Supplementary Tables S1B and S1C) supports such notion. Reducing the levels of many targets including CCNA2, miR-124 may alter the cell cycle.

Recently, it has been shown that E2F3 is a target of miR-125b and CCNA2 is regulated by E2F3 [32]. Expression of miR-125b is decreased in STHdh^{Q111}/Hdh^{Q111} cells [14]. Thus, miR-125b could also contribute to increased expression of CCNA2 through E2F3 in STHdh^{Q111}/Hdh^{Q111} cells.

CCNA2 is known to control S phase by initiating DNA synthesis interacting with CDK2 [33]. Ectopic overexpression of CCNA2 could trigger checkpoint response [34] and subsequently increases S-phase population in mammalian cells [35]. We also observed, CCNA2 overexpression increases CHK1 expression in STHdh^{Q7}/Hdh^{Q7} cells.

Decreased miR-124 expression in cell, animal model and HD brains [10] as well as increased CCNA2 and other known target proteins like CDK2, CDK4 [36] may reactivate cell cycle. Further experiments are necessary to elucidate the fate of cells in S phase. In conclusion, decreased expression of miR-124 in cell model and animal model of HD may reactivate cell cycle targeting many regulatory proteins including CCNA2.

Acknowledgments

We thank Dr. Marcy E. MacDonald of Massachusetts General Hospital, USA for providing STHdh^{Q7}/Hdh^{Q7} and STHdh^{Q111}/Hdh^{Q111} cells. We would like to acknowledge Dr. Sumanta Basu and Sutapa Saha for their assistance in Flow cytometry analysis. This work was supported by institutional grant from the Department of Atomic energy, Government of India.

Appendix A. Supplementary data

Supplementary data associated with this article can be found, in the online version, at http://dx.doi.org/10.1016/j.bbrc.2013.06.041.

References

[1] A.M. Cheng, M.W. Byrom, J. Shelton, et al., Antisense inhibition of human miRNAs and indications for an involvement of miRNA in cell growth and apoptosis, Nucleic Acids Res. 33 (2005) 1290–1297.
[2] Y. Tay, J. Zhang, A.M. Thomson, et al., MicroRNAs to Nanog, Oct4 and Sox2 coding regions modulate embryonic stem cell differentiation, Nature 455 (2008) 1124–1128.
[3] A. Blakaj, H. Lin, Piecing together the mosaic of early mammalian development through microRNAs, J. Biol. Chem. 283 (2008) 9505–9508.
[4] G. Stefani, F.J. Slack, Small non-coding RNAs in animal development, Nat. Rev. Mol. Cell Biol. 9 (2008) 219–230.
[5] N. Cloonan, M.K. Brown, A.L. Steptoe, et al., The miR-17-5p microRNA is a key regulator of the G1/S phase cell cycle transition, Genome Biol. 9 (2008) R127.
[6] H. Xia, Y. Qi, S.S. Ng, et al., MicroRNA-15b regulates cell cycle progression by targeting cyclins in glioma cells, Biochem. Biophys. Res. Commun. 380 (2009) 205–210.
[7] L. Xia, D. Zhang, R. Du, et al., MiR-15b and miR-16 modulate multidrug resistance by targeting BCL2 in human gastric cancer cells, Int. J. Cancer 123 (2008) 372–379.
[8] A. Ruepp, A. Kowarsch, D. Schmidl, et al., PhenomiR: a knowledgebase for microRNA expression in diseases and biological processes, Genome Biol. 11 (2010) R6.
[9] M. Sinha, J. Ghose, E. Das, et al., Altered microRNAs in STHdh(Q111)/Hdh(Q111) cells: miR-146a targets TBP, Biochem. Biophys. Res. Commun. 396 (2010) 742–747.
[10] R. Johnson, C. Zuccato, N.D. Belyaev, et al., A microRNA-based gene dysregulation pathway in Huntington's disease, Neurobiol. Dis. 29 (2008) 438–445.
[11] E. Marti, L. Pantano, M. Banez-Coronel, et al., A myriad of miRNA variants in control and Huntington's disease brain regions detected by massively parallel sequencing, Nucleic Acids Res. 38 (2010) 7219–7235.
[12] A.N. Packer, Y. Xing, S.Q. Harper, et al., The bifunctional microRNA miR-9/miR-9* regulates REST and CoREST and is downregulated in Huntington's disease, J. Neurosci. 28 (2008) 14341–14346.
[13] M. Sinha, J. Ghose, N.P. Bhattarcharyya, Micro RNA -214,-150,-146a and-125b target Huntingtin gene, RNA Biol. 8 (2011) 1005-1021.
[14] J. Ghose, M. Sinha, E. Das, et al., Regulation of miR-146a by RelA/NFkB and p53 in STHdh(Q111)/Hdh(Q111) cells, a cell model of Huntington's disease, PLoS ONE 6 (2011) e23837.
[15] M. Sinha, S. Mukhopadhyay, N.P. Bhattacharyya, Mechanism(s) of alteration of micro RNA expressions in Huntington's disease and their possible contributions to the observed cellular and molecular dysfunctions in the disease, Neuromolecular Med. 14 (2012) 221–243.
[16] W. Wang, B. Bu, M. Xie, et al., Neural cell cycle dysregulation and central nervous system diseases, Prog. Neurobiol. 89 (2009) 1–17.
[17] K. Herrup, Y. Yang, Cell cycle regulation in the postmitotic neuron: oxymoron or new biology?, Nat Rev. Neurosci. 8 (2007) 368–378.
[18] J. Folch, F. Junyent, E. Verdaguer, et al., Role of cell cycle re-entry in neurons: a common apoptotic mechanism of neuronal cell death, Neurotox. Res. 22 (2012) 195–207.
[19] C. Pelegri, J. Duran-Vilaregut, J. del Valle, et al., Cell cycle activation in striatal neurons from Huntington's disease patients and rats treated with 3-nitropropionic acid, Int. J. Dev. Neurosci. 26 (2008) 665–671.
[20] F. Trettel, D. Rigamonti, P. Hilditch-Maguire, et al., Dominant phenotypes produced by the HD mutation in STHdh(Q111) striatal cells, Hum. Mol. Genet. 9 (2000) 2799–2809.
[21] S. Raychaudhuri, M. Sinha, D. Mukhopadhyay, et al., HYPK, a Huntingtin interacting protein, reduces aggregates and apoptosis induced by N-terminal Huntingtin with 40 glutamines in Neuro2a cells and exhibits chaperone-like activity, Hum. Mol. Genet. 17 (2008) 240–255.
[22] M. Datta, A. Choudhury, A. Lahiri, et al., Genome wide gene expression regulation by HIP1 Protein Interactor, HIPPI: prediction and validation, BMC Genomics 12 (2011) 463.
[23] K.R. Choudhury, S. Raychaudhuri, N.P. Bhattacharyya, Identification of HYPK-interacting proteins reveals involvement of HYPK in regulating cell growth, cell cycle, unfolded protein response and cell death, PLoS ONE 7 (2012) e51415.
[24] M. Maheshwari, A. Samanta, S.K. Godavarthi, et al., Dysfunction of the ubiquitin ligase Ube3a may be associated with synaptic pathophysiology in a mouse model of Huntington disease, J. Biol. Chem. 287 (2012) 29949–29957.
[25] R. Nogales-Cadenas, P. Carmona-Saez, M. Vazquez, et al., GeneCodis: interpreting gene lists through enrichment analysis and integration of diverse biological information, Nucleic Acids Res. 37 (2009) W317–W322.
[26] S. Gines, I.S. Seong, E. Fossale, et al., Specific progressive cAMP reduction implicates energy deficit in presymptomatic Huntington's disease knock-in mice, Hum. Mol. Genet. 12 (2003) 497–508.
[27] C. Zuccato, N. Belyaev, P. Conforti, et al., Widespread disruption of repressor element-1 silencing transcription factor/neuron-restrictive silencer factor occupancy at its target genes in Huntington's disease, J. Neurosci. 27 (2007) 6972–6983.
[28] C.L. Benn, T. Sun, G. Sadri-Vakili, et al., Huntingtin modulates transcription, occupies gene promoters in vivo, and binds directly to DNA in a polyglutamine-dependent manner, J. Neurosci. 28 (2008) 10720–10733.

[29] M. Turmaine, A. Raza, A. Mahal, et al., Nonapoptotic neurodegeneration in a transgenic mouse model of Huntington's disease, Proc. Natl. Acad. Sci. USA 97 (2000) 8093–8097.
[30] M. Datta, N.P. Bhattacharyya, Regulation of RE1 protein silencing transcription factor (REST) expression by HIP1 protein interactor (HIPPI), J. Biol. Chem. 286 (2011) 33759–33769.
[31] M.S. Ebert, P.A. Sharp, Roles for microRNAs in conferring robustness to biological processes, Cell 149 (2012) 515–524.
[32] L. Huang, J. Luo, Q. Cai, et al., MicroRNA-125b suppresses the development of bladder cancer by targeting E2F3, Int. J. Cancer 128 (2011) 1758–1769.
[33] M. Pagano, R. Pepperkok, F. Verde, et al., Cyclin A is required at two points in the human cell cycle, EMBO J. 11 (1992) 961–971.
[34] S. Tane, T. Chibazakura, Cyclin A overexpression induces chromosomal double-strand breaks in mammalian cells, Cell Cycle 8 (2009) 3900–3903.
[35] T. Chibazakura, S.G. McGrew, J.A. Cooper, et al., Regulation of cyclin-dependent kinase activity during mitotic exit and maintenance of genome stability by p21, p27, and p107, Proc. Natl. Acad. Sci. USA 101 (2004) 4465–4470.
[36] M.R. Fernandez-Fernandez, I. Ferrer, J.J. Lucas, Impaired ATF6alpha processing, decreased Rheb and neuronal cell cycle re-entry in Huntington's disease, Neurobiol. Dis. 41 (2011) 23–32.